Eur. Phys. J. B **27**, 459–466 (2002)
DOI: 10.1140/epjb/e2002-00178-9

THE EUROPEAN PHYSICAL JOURNAL B

Hole doping by Li substitution and antiferromagnetism in $YBa_2Cu_3O_y$ studied by neutron powder diffraction measurements

F. Maury[1,a], I. Mirebeau[2], M. Nicolas-Francillon[3], and F. Bourée[2]

[1] Laboratoire des Solides Irradiés, École Polytechnique, 91128 Palaiseau Cedex, France
[2] Laboratoire Léon Brillouin (CEA-CNRS), CEA/Saclay, 91191 Gif-sur-Yvette Cedex, France
[3] Laboratoire de Physique du Solide, ESPCI, 10 rue Vauquelin, 75231 Paris Cedex 05, France

Received 31 October 2001 and Received in final form 6 March 2002
Published online 25 June 2002 –

Abstract. The magnetic structure of tetragonal insulating $YBa_2Cu_{3-x}Li_xO_y$ has been studied as a function of x and y. The Néel temperature and the mean ordered magnetic moment on the Cu2 sites were determined by neutron powder diffraction measurements. The decrease of these two parameters as compared to $YBa_2Cu_3O_6$ is much stronger for lithium than for zinc substitution. The difference is quantitatively explained by the presence of holes created in the CuO_2 planes. These holes arise from the substitution of plane Cu^{2+} by Li^+. We suggest an explanation why such holes are not seen for the same substitution of plane Cu^{2+} by Li^+ in orthorhombic superconducting $YBa_2Cu_{3-x}Li_xO_{7-\delta}$.

PACS. 74.72.Bk Y-based cuprates – 75.50.Ee Antiferromagnetics

1 Introduction

This work completes a study of the Li effect on the antiferromagnetic (AF) structure of tetragonal $YBa_2Cu_{3-x}Li_xO_y$.

$YBa_2Cu_3O_y$ is tetragonal, insulating and antiferromagnetic for $y < 6.4$. The ordered magnetic moments are carried by the Cu^{2+} ions in the CuO_2 planes [1,2]. (In the following, Cu2/Li2 will refer to Cu/Li ions sitting on CuO_2 plane sites and Cu1/Li1 to Cu/Li ions on Cu chain sites.)

We have shown [3] that the Li substitution decreases both the ordering temperature T_N and the mean ordered magnetic moment μ, in the same way as oxygen doping. This result can be simply interpreted by considering that the lithium substitution creates holes in the CuO_2 planes, which holes are responsible for the destruction of the in-plane AF order.

Such holes are indeed expected to be created by the mere replacement of $Cu2^{2+}$ by $Li2^+$ ions. Yet, in orthorhombic $YBa_2Cu_{3-x}Li_xO_{7-\delta}$, NMR results of Bobroff *et al.* [4] show that no extra holes are localized near the $Li2^+$ ions: any additional hole must delocalize in the band of carriers of the CuO_2 planes. But resistivity measurements [5] show that up to $x = 0.25$, the Li substitution increases the resistivity ρ and decreases the critical temperature T_c without changing much the shape of the $\rho(T)$ curve, thus suggesting that the carrier concentration is not modified by the substitution. This is confirmed by the fact that Li and Zn induce similar reductions of T_c [4]. The experiments thus indicate that, contrary to what is expected, the Li substitution in $YBa_2Cu_{3-x}Li_xO_{7-\delta}$, does not create any extra hole, either localized or mobile. These experimental results look in contradiction also with what is expected if one apical oxygen is lost per substituted Li2, as suggested by our neutron data [6], since in that case, the Li2 substitution should globally suppress (and not create) one hole per Li.

In tetragonal $YBa_2Cu_{3-x}Li_xO_{6+\epsilon}$, the neutron results seem to indicate that the apical oxygen (about one oxygen per substituted Li2) is not lost but shifted to a chain site; as a consequence, the holes brought in by the Li2 ions could be localized on chain coppers ($Cu1^+$ becoming $Cu1^{2+}$) and not hinder much the AF ordering in the CuO_2 planes. The strong AF suppression that is observed could then result from holes transferred in the CuO_2 planes from extra chain oxygens neighbouring these $Cu1^{2+}$ or $Li1^+$ ions. The present experiment was aimed at ascertaining the origin of the holes created in the CuO_2 planes by the Li substitution.

We briefly recall in Section 2 our experimental conditions. We present in Section 3 the sample characterization (residual impurities, oxygen and lithium concentration) and in Section 4 the AF order determined by neutron powder diffraction measurements. The results are discussed in Section 5.

[a] e-mail: francoise.maury@polytechnique.fr

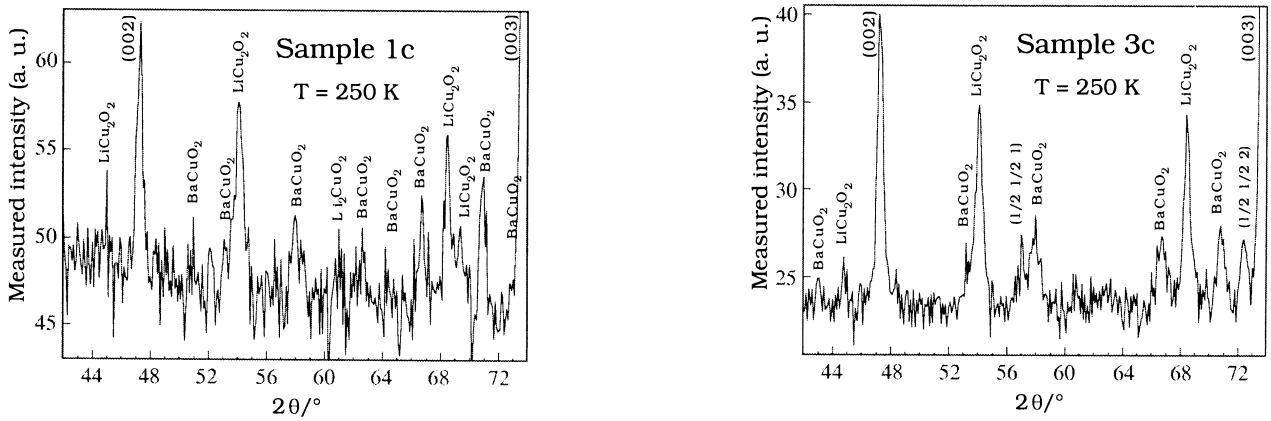

Fig. 1. Neutron diffraction data measured with the G6-1 spectrometer at $T = 250$ K.

2 Experimental

The samples were prepared by the usual solid state reaction as described in reference [5]. Just before the present experiment, two samples already studied in reference [3], samples 1b and 3, which had been annealed in argon at 750 °C, were annealed in argon at 800 °C and are thereafter called samples 1c and 3c.

The detailed crystallographic structure of the samples was determined by neutron powder diffraction measurements carried out at room temperature on the high resolution powder diffractometer 3T2 of the Laboratoire Léon Brillouin with $\lambda = 1.2251$ Å and in the range of scattering angles $7° \leq 2\theta \leq 125°$. The data were analyzed using the Fullprof program [7]. Lattice parameters, atom coordinates, oxygen and Cu/Li site occupancies, isotropic thermal factors, peak shape and width, preferred orientation, scale factor and background were refined.

The magnetic structure of the samples was determined by neutron powder diffraction measurements carried out at various temperatures on the high flux diffractometer G6-1 of the Laboratoire Léon Brillouin with $\lambda = 4.738$ Å and in the range $20° < 2\theta < 120°$ for sample 1c and $5° < 2\theta < 147°$ for sample 3c. The experimental set up was slightly different below and above room temperature ($T \geq 310$ K). The signal of the sample holder was registered at 220 K for sample 1c and 300 K for sample 3c, slightly below T_N in each case, and subtracted from the sample measured spectra. The obtained spectra were refined using the Fullprof program: lattice parameters, atom coordinates, peak width, scale factor, background and mean ordered magnetic moment on the Cu2 sites were refined, the other parameters being taken as determined by the 3T2 experiment. The temperature dependence of the mean ordered moment was also deduced from a Gaussian fit of the two (1/2 1/2 1) and (1/2 1/2 2) magnetic peaks.

3 Sample characterisation

3.1 Residual impurities

Figure 1 shows the G6-1 neutron diffraction spectra measured at $T = 250$ K for the two samples 1c and 3c. The scale is much enlarged since with the units of Figure 1, the YBCO (001) peak reaches a maximum intensity of 1800. The extra peaks clearly distinguishable from the background all belong either to $LiCu_2O_2$ [8] or to $Ba_{44}Cu_{48}(CO_3)_6O_{81+x}$ [9] (called "BaCuO2" hereafter). The spectra measured for samples 1b and 3 are displayed in Figure 1 of reference [3].

The ratio of the total integrated intensity of the impurity peaks to that of the YBCO peaks, which should be of the order of the impurity volumic fraction, has been calculated for each of the residual impurities. For $BaCuO_2$, it amounts to $\approx 2.5\%$ in sample 1c and $\approx 0.5\%$ in sample 3c. For $LiCu_2O_2$, it is $\approx 0.5\%$ in both samples. Li_2CuO_2 [10], observed in sample 1b, is no longer observed in 1c: it has been entirely reduced into $LiCu_2O_2$.

3.2 Oxygen concentration

The excess of charge on the Cu ions as compared to Cu^+ was determined by iodometric titration and the oxygen content deduced from electrical neutrality [5]. The oxygen concentration per unit formula so determined, is called "experimental" and given in Table 1. The uncertainty on $y_{\rm exp}$ is ± 0.04. We checked (see Ref. [3]) that the presence of a few percent of residual "$BaCuO_2$", Li_2CuO_2 or $Li_2Cu_2O_2$ change these values negligibly as compared to the experimental uncertainty.

The oxygen concentration is also deduced from the neutron diffraction data of the 3T2 experiment. The data were analyzed as follows (for more details see Ref. [6]).

First (model I), we refined the number of oxygens on both the apical (O1) and chain (O4) sites. The corresponding value of y is called $y_{\rm calc}$. We see that $y_{\rm calc}$ is then always very close to $y_{\rm exp}$.

We also refined the neutron data by constraining n(O1) to remain equal to 2. The refined value of n(O4) is not changed significantly, which leads to a too high value of $y_{\rm calc}$ as compared to $y_{\rm exp}$. Consequently, we had to constrain n(O4) in addition, so that $y_{\rm calc} = y_{\rm exp}$. When $n(\mathrm{O4}) \neq 0$, this yields a refined value of the O4 thermal factor much to small to bear any physical meaning. In such cases, we also constrained B(O4) to remain equal to 1.5, slightly larger than B(O1). The refined values of the

Table 1. Structural parameters obtained by Rietveld refinement of neutron data for tetragonal $YBa_2Cu_{3-x}Li_xO_y$. O_{apex} = O1(0, 0, z), O2 (0.5,0,z), O_{chain} = O4 (x,0.5,0), Cu1 (0,0,0), Cu2 (0,0,z). For each atomic position, n is the site occupancy and B the thermal factor (given in $Å^2$). Numbers in brackets correspond to fixed values. Numbers in parentheses which follow refined parameters represent one standard deviation in the last digit. The full set of parameters is available on request.

	Model	y_{calc}	x_{calc}	n(Li1)	n(Li2)	B(Cu1)	B(Cu2)	n(O1)	B(O1)	B(O4)	R_B (%)	R_{wp} (%)
Sample 1b	I	6.16 (3)	0.11 (2)	0.025 (7)	0.085 (9)	0.83 (4)	0.46 (3)	1.91 (2)	.94 (5)	1.5 (6)	3.76	5.95
y_{exp} = 6.18 (4)	II	[6.18]	0.10 (2)	0.027 (7)	0.070 (9)	0.77 (5)	0.46 (3)	[2.00]	1.12 (3)	[1.5]	3.97	6.02
R_{exp} = 4.26 %												
Sample 1c	I	6.01 (3)	0.11 (2)	0.005 (8)	0.104 (10)	0.94 (5)	0.39 (3)	1.89 (2)	0.87 (5)	1.6 (10)	3.67	6.00
y_{exp} = 5.99 (4)	II	[6.00]	0.09 (2)	0.006 (8)	0.087 (10)	0.87 (5)	0.39 (3)	[2.00]	1.06 (3)	-	3.91	6.11
R_{exp} = 4.74 %												
Sample 3	I	6.03 (2)	0.11 (1)	0.013 (4)	0.100 (6)	0.91 (3)	0.41 (2)	1.91 (1)	0.95 (3)	3 (2)	3.21	4.18
x_{exp} = 0.09 (2)												
y_{exp} = 6.04 (4)	II	[6.04]	0.10 (1)	0.013 (4)	0.085 (6)	0.86 (3)	0.41 (2)	[2.00]	1.12 (2)	[1.5]	3.46	4.27
R_{exp} = 2.58 %												
Sample 3c	I	6.02 (3)	0.09 (1)	0.012 (6)	0.078 (8)	0.91 (4)	0.45 (2)	1.90 (2)	0.93 (4)	3 (2)	3.11	4.74
y_{exp} = 5.99 (4)	II	[6.00]	0.08 (1)	0.014 (6)	0.062 (7)	0.85 (4)	0.46 (2)	[2.00]	1.09 (3)	-	3.27	4.85
R_{exp} = 3.80 %												

various parameters then obtained, are given in Table 1 with the label model II.

The fit quality is only slightly different for the two models and not sufficient to discard one model. That model I yields a refined value of y equal to the experimental one for all studied samples could be a mere although unlikely coincidence.

3.3 Lithium concentration and distribution

The Li and Cu contents were determined by emission plasma spectrometry analysis. Among the four samples of the present study, the analysis was performed only for sample 3. It yielded a lithium concentration per unit formula, $x_{exp} = 0.09 \pm 0.02$ and a copper concentration of 2.89 ± 0.02. Due to the presence of a small fraction of residual $LiCu_2O_2$ ($f_{LiCu_2O_2} \approx 0.3\%$), the value of x_{exp} may be slightly overestimated.

Values of x are also deduced from the refinement of the neutron data. The refinement of n(Li1) and n(Li2) is made possible by the very different values of the Li and Cu scattering lengths (−1.90 fm and +7.72 fm respectively). The refined values of x (x_{calc}) are given in Table 1. If, for sample 3, we compare x_{calc} with x_{exp}, we see that the two values are consistent, given the uncertainty of both determinations.

If we now compare sample 3c and sample 3, we see that the 800 °C anneal that has transformed sample 3 in sample 3c has reduced n(Li2) without changing n(Li1), thus resulting in a small decrease of x. This decrease is confirmed by the G61 experiment which evinces an increase of residual $LiCu_2O_2$ which can have formed but at the expense of the YBCO-Li phase.

In the case of sample 1, the Li and Cu contents were determined by spectrometry on the orthorhombic precursor of samples 1b and 1c. The lithium concentration was $x_{exp} = 0.115 \pm 0.02$ and the copper concentration 2.89 ± 0.02. Due to the presence of residual Li_2CuO_2 ($f_{Li_2CuO_2} \approx 1\%$), this value of x_{exp} must be overestimated, but no reliable correction of x can be estimated from the integrated area of the three observed Li_2CuO_2 peaks.

If we now look at the calculated values of n(Li2), we see that sample 3c has the lowest n(Li2). To corroborate this point, powder samples 1c and 3c were annealed together at 480 °C, after the neutron experiment, and their magnetic transition onset temperature measured. It is 54 K for sample 1c and 58 K for 3c, in good agreement with a n(Li2) value slightly larger for sample 1c than for 3c. Assuming that the Li substitution does not create any extra hole in orthorhombic $YBa_2Cu_3O_7$ and consequently that the Li effect is a mere T_c dilution effect similar to that of Zn, these measured values are compared to that of the literature for Zn substitution, in Figure 2. The T_c values are not determined with a precision better than ± 4 K due to the broadness of the transition, but the accuracy on the difference between the T_c of samples 1c and 3c is much better.

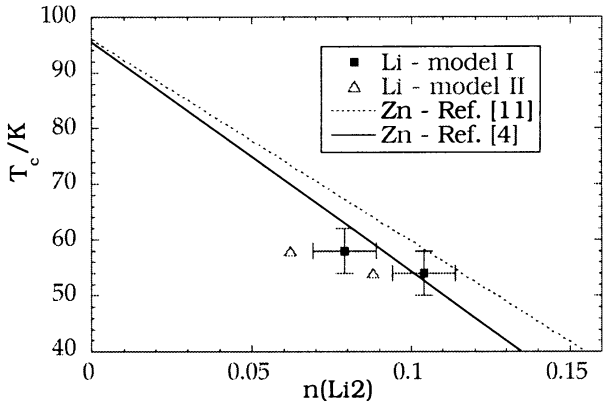

Fig. 2. Superconducting transition temperature as a function of n(Li2/Zn). The uncertainty on n(Li2), shown for model I, is similar for both models.

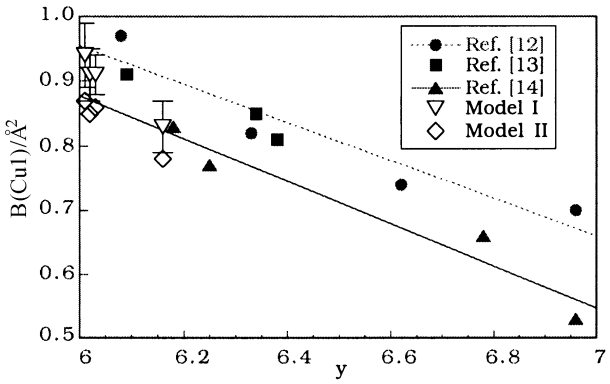

Fig. 3. Thermal factor of the Cu1 site as a function of y. The full symbols are for $YBa_2Cu_3O_y$, the open ones for $YBa_2Cu_{3-x}Li_xO_y$. The error bars, shown for model I, are similar for both models.

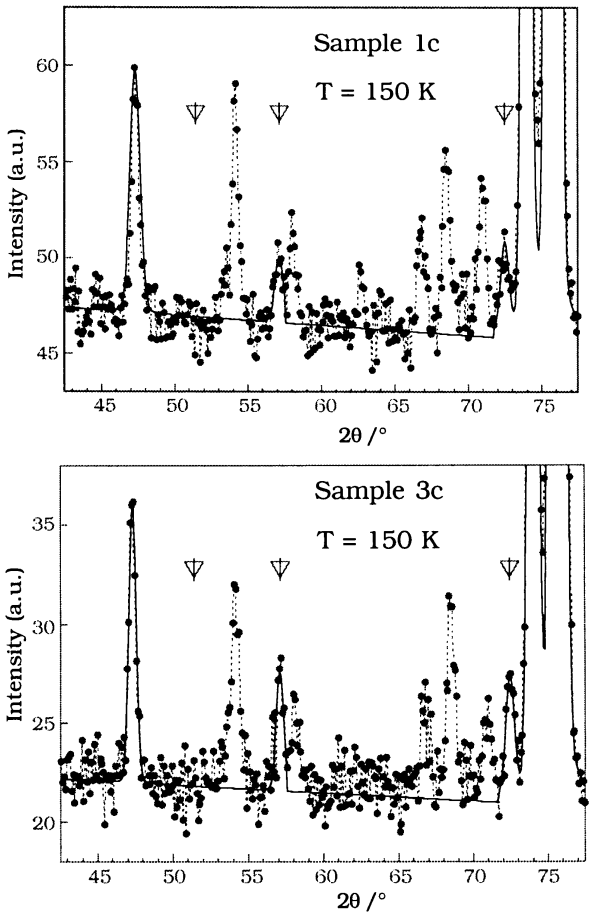

Fig. 4. Neutron diffraction data measured at $T = 150$ K with the G6-1 spectrometer. The points and dotted line represent the experimental data. The barred triangles show the position of the magnetic peaks (1/2 1/2 l) for $l = 0, 1$ and 2. The solid line is the calculated profile; sample 1c: $\mu/\mu_B = 0.29$; sample 3c: $\mu/\mu_B = 0.35$.

If we now look at n(Li1), we see that sample 1c has the lowest n(Li1) and sample 1b the largest n(Li1). The determination of n(Li1) is supported by the fact that the refined values of the thermal factor B(Cu1) are found in good agreement with the values in the literature for unsubstituted YBaCuO [12–14]. B(Cu1) is slightly smaller with model II than with model I but the difference is small and not larger than the dispersion in the values of the literature (*cf.* Fig. 3).

These values of n(Li1) and n(Li2) have been refined with the constraint of a full occupancy of the Cu sites; the spectroscopy analysis gives indeed a total number of Cu and Li per unit formula equal to 3.00 within the experimental uncertainties (0.04), as long as $x < 0.25$. Moreover, assuming for example, 1% of vacancy on the Cu1 sites, would entail a n(Li1) decrease of 0.008, whatever the sample or the model. We thus think that a significant meaning can reliably be attached to the relative values of n(Li1) and n(Li2), if not to their absolute values since these depend on the model. The three samples with $y = 6.0$, have similar n(Li1) and among them, sample 3c has the lowest n(Li2).

4 Magnetic structure

4.1 Néel temperature

Figure 4 shows the neutron diffraction spectra measured with the G6-1 spectrometer for samples 1c and 3c at $T = 150$ K. They display, together with the various impurity peaks, two diffraction peaks which can be indexed (1/2 1/2 1) and (1/2 1/2 2). These peaks which are clearly visible at low temperature and disappear at high temperature, arise from the doubling of the magnetic unit cell along the a and b axes, due to the AF order in the CuO_2 planes. They are not seen on the spectra measured, for sample 1c, at $T \geq 250$ K (see Fig. 1) and for sample 3c, at $T \geq 330$ K, which shows that they do stem from magnetism and not from residual impurities.

To determine T_N, we calculated the integrated intensity of the (1/2 1/2 1) magnetic peak, deduced from a Gaussian fit of both YBCO (1/2 1/2 1) peak and "$BaCuO_2$" (3 2 1) peak, in the range $56° < 2\theta < 58.8°$,

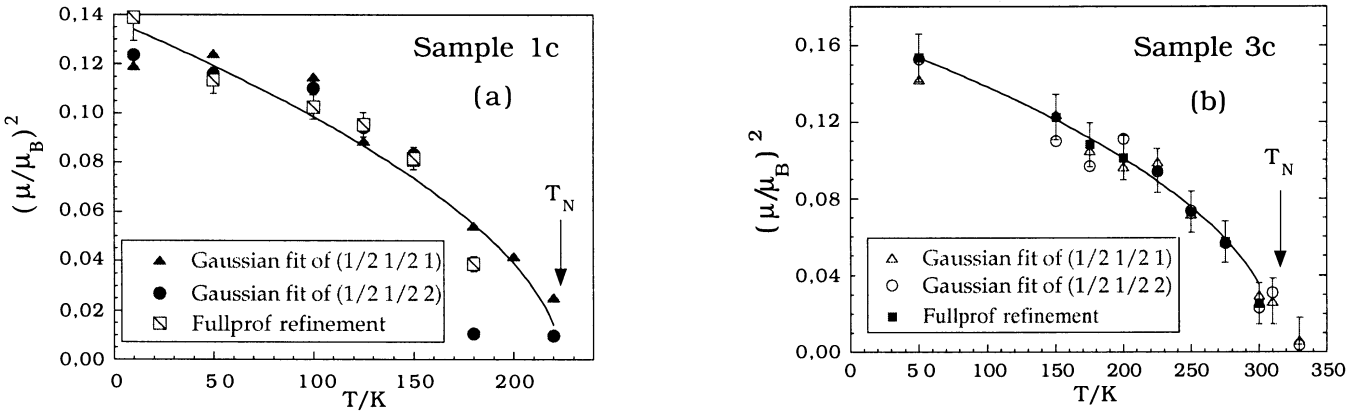

Fig. 5. Square of the mean ordered magnetic moment on Cu2 sites determined either by the refinement of the neutron data or by a Gaussian fit of the (1/2 1/2 1) and (1/2 1/2 2) peaks with normalization to the Fullprof values at $T = 50$ K. The solid line is calculated with $\mu = \mu_0\ (1 - T/T_N)^{\beta}$. (a) sample 1c: $\mu_0/\mu_B = 0.37$, $T_N = 224$ K, $\beta = 0.28$. (b) sample 3c: $\mu_0/\mu_\beta = 0.41$, $T_N = 314$ K, $\beta = 0.25$.

Table 2. Deduced ordering temperature as a function of the Li concentration on Cu1 and Cu2 sites.

			model I		model II	
Sample	y_{exp}	T_N/K	n(Li1)	n(Li2)	n(Li1)	n(Li2)
3c	5.99 (4)	315 (15)	0.012 (6)	0.078 (8)	0.014 (6)	0.062 (7)
3	6.04 (4)	245 (15)	0.013 (4)	0.100 (6)	0.013 (4)	0.085 (6)
1c	5.99 (4)	225 (15)	0.005 (8)	0.104 (10)	0.006 (8)	0.087 (10)
1b	6.18 (4)	150 (30)	0.025 (7)	0.085 (9)	0.027 (7)	0.070 (9)

and that of the (1/2 1/2 2) magnetic peak, deduced from a Gaussian fit of both "$BaCuO_2$" (4 2 0) peak and YBCO (1/2 1/2 2) peak, in the range $70° < 2\theta < 72.7°$. The obtained values are displayed in Figure 5.

Table 2 gives the T_N values deduced for our four samples. If we compare the three samples with y = 6.0 (samples 3c, 3 and 1c), we see that T_N is definitely a decreasing function of n(Li2) and not of n(Li1): the comparison of samples 3 and 3c shows that T_N does depend strongly on n(Li2); the comparison of samples 3c and 1c shows that the T_N decrease cannot be attributed to a n(O4) and/or n(Li1) increase, which contradicts our assumption that the AF suppression could result from holes transferred in the CuO_2 planes from extra chain oxygens neighbouring $Li1^+$ ions.

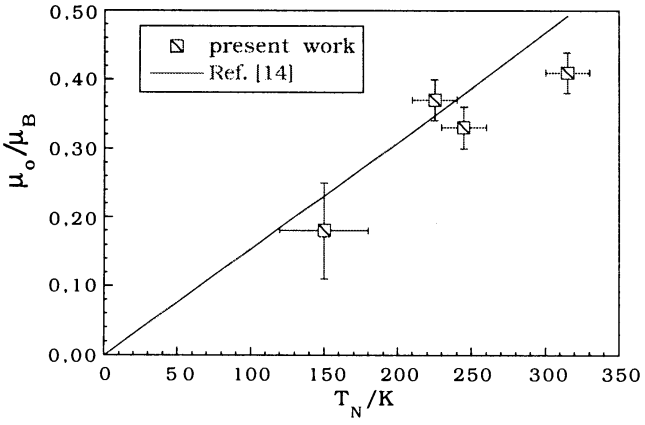

Fig. 6. Mean ordered magnetic moment at low temperature as a function of T_N.

4.2 Mean ordered magnetic moment

The mean ordered magnetic moment on the Cu2 sites was deduced from the refinement of the G6-1 data for $40° < 2\theta < 90°$. (The fits to the experimental data obtained for samples 1c and 3c at $T = 150$ K are displayed in Fig. 4 and the refined values of μ/μ_B as a function of the temperature in Fig. 5.)

If we plot the value of the low temperature ordered moment as a function of the ordering temperature (Fig. 6), we see that our values roughly fall on the same curve as those of Rossat-Mignod *et al.* [15] for unsubstituted YBCO. Moreover, the shape of the $\mu(T)$ curves (given by the value of the β parameter) is similar, for similar values of T_N, in our experiment and that of reference [15].

5 Discussion

The observed weakening of the 3D AF order in $YBa_2Cu_3O_y$ with increasing y, stems from hole doping. In unsubstituted $YBa_2Cu_3O_y$ with $6 < y < 6.2$, the doped holes are localized on the Cu1 neighbours of the chain oxygens and do not affect the AF order [15]. The reduction of both T_N and μ_0 starts around $y = 6.2$, when a few mobile holes begin to be created in the CuO_2 planes.

The similarity between our results and those for $YBa_2Cu_3O_{6+\epsilon}$ indicates that the main effect of the Li substitution is a hole doping effect. The values listed in Table 2 show that these holes result from the substitution of the Cu2 ions and not of Cu1 ions. This is indeed what is expected if a Li^+ merely substitutes for a $Cu2^{2+}$.

5.1 Interpretation of the data with model II

In model II, the Li substitution is assumed to take place without any oxygen loss; the interpretation of the results is then straightforward: for each Li^+ substituted for a $Cu2^{2+}$, one hole is created in the CuO_2 planes, while the substitution of a Li^+ for a chain $Cu1^+$ does not modify the hole concentration. The number of holes induced by the substitution is thus equal to the number of substituted Li2.

The black triangles in Figure 7 show T_N as a function of p, number per unit formula of holes created in the CuO_2 planes: $p = n(\mathrm{Li2})$. One sees that for the three samples with $y \approx 6.0$, T_N is a smooth function of p. In sample 1b, with $y = 6.18$, extra plane holes are created by oxygen doping and the total number of plane holes has to be calculated by adding to $n(\mathrm{Li2})$ the number of doped holes. At the moment, let us discard this sample and compare our results to those of Sidis *et al.* [16] for $YBa_2Cu_{2.92}Zn_{0.08}O_{6.2}$.

The Zn substitution does not modify the hole concentration and results in a decrease of the ordering temperature which is small (≈ 60 K for $x_{\mathrm{Zn}} = 0.08$) and about constant in a large domain of p [16]. This decrease, proportional to the solute (or missing magnetic moment) concentration, is interpreted as a mere dilution effect which adds to the effect of oxygen doping [16–18].

The Li2 concentration in our samples being of the same order of magnitude as that of Zn in the sample of Sidis *et al.*, one thus expects the dilution effect to be a mere constant decrease of T_N of about 60 K. The decrease of T due to Li-hole doping must then be roughly given by the dotted line of Figure 7.

The Li-hole effect can then be compared to the doped hole effect in unsubstituted YBaCuO, where T_N is known as a function of y, provided p is known as a function of y. Unfortunately, no reliable estimation of p as a function of y can be found in the literature: for $y = 0.4$ for example, p is found to vary between 0.06 [19] and 0.4 [20]. Alternatively, one can assume that the Li-holes and the doped holes have the same effect on T_N and deduce p as a function of y. Taking T_N as a function of y as given by reference [15]

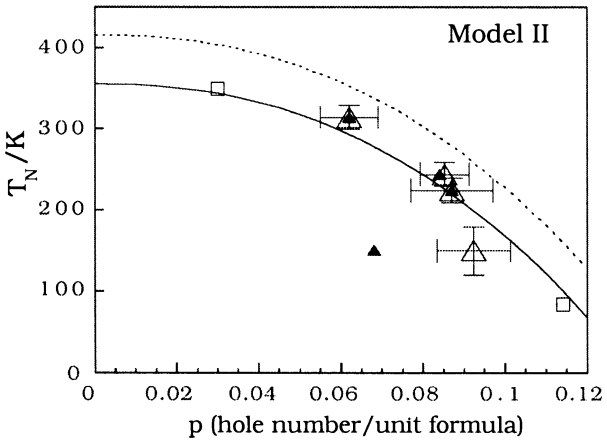

Fig. 7. T_N as a function of the hole concentration. p is the number of holes created in the CuO2 planes, per unit formula. Black triangles: $p = n(\mathrm{Li2})$. Open triangles: $p = n(\mathrm{Li2}) + p_y$, where p_y is the hole number due to oxygen doping. Solid line: eye-fit to the data. Dotted line: T_N as a function of p, after subtraction of the dilution effect. Squares: tetragonal $YBa_2Cu_{2.92}Zn_{0.08}O_y$ [16].

(and as a function of p as given by the dotted line of Figure 7), one gets: $p = 0.75\ (y\text{-}6)^2$.

This is 3/4 of what would correspond to a random distribution of the extra oxygens on the O4 sites, indicative of a slightly repulsive oxygen order. For $y = 6.4$, it gives $p = 0.12$, *i.e.* twice the value of reference [19], a value near what is currently admitted [21].

With this formula, one can estimate the hole number for the two $YBa_2Cu_{2.92}Zn_{0.08}O_{6+\varepsilon}$ samples of Sidis *et al.* [16] and the total hole number for sample 1b (open symbols in Fig. 7). All data then do fall on the same curve within the experimental uncertainties, although T_N is still a little lower than expected for sample 1b.

Due to our crude estimate of $T_N(p)$ and to the dispersion in the $T_N(y)$ curves (see [15,22,23]), this agreement is more an indication that the Li-hole effect cannot be distinguished from the doped hole effect than of the exactness of the $p(y)$ formula.

To conclude, one can consider that model II explains well and simply the results of the G6-1 experiment: the substitution of a Li2 for a Cu2 suppresses a spin and creates a hole in the CuO_2 plane; these two effects add to decrease both T_N and the mean ordered magnetic moment on the Cu2 sites.

The effect of the Li-holes appears quantitatively similar to that of the mobile doped holes. Yet, it cannot be ascertained whether the Li-holes are mobile rather than localized, since there is no consensus in the literature as whether localized holes are more destructive to the AF order than mobile ones.

5.2 Interpretation of the data with model I

In model I, for each substituted Li2, one apical oxygen is shifted to a chain site. Since the substitution has to bring

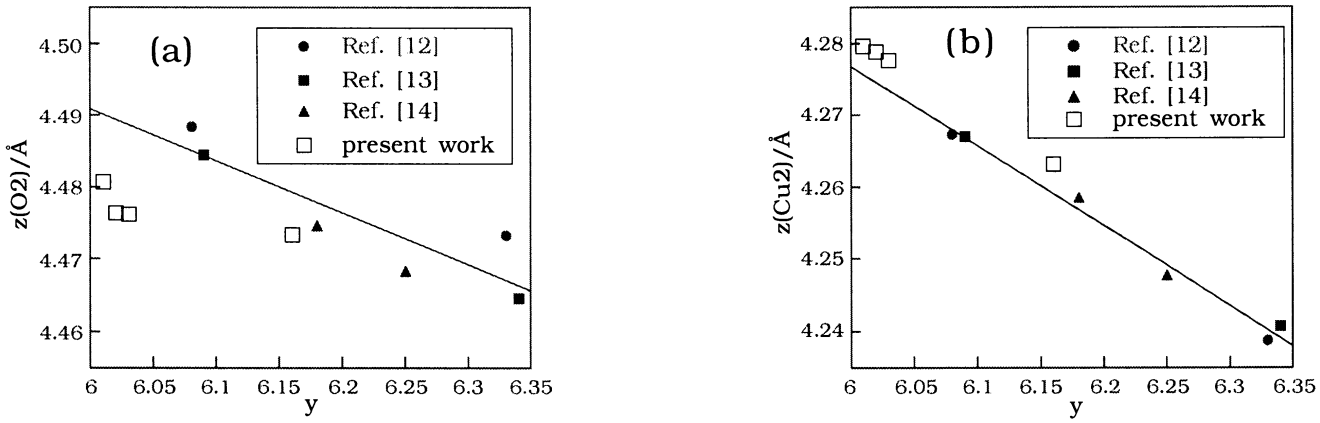

Fig. 8. z(O2) (a) and z(Cu2) (b), deduced from the 3T2 experiment, as a function of y for unsubstituted (full symbols) and Li-substituted (open squares) YBaCuO.

a hole in the CuO_2 plane in order to explain the present results, the displacement of the apical oxygen to a chain site must not change the charge state of the nearby Cu1 ions, instead of which the Li-hole would be localized on this Cu1 and not in the CuO_2 plane. In this model, an O1 vacancy stands between a $Li2^+$ and a $Cu1^+$.

Then a figure quite similar to Figure 7 can be drawn, where the efficiency of a given number of holes in abating T_N is but a little smaller, since n(Li2) is a little larger with model I than with model II. The $p(y)$ formula is slightly changed and the data point for sample 1b comes in perfect agreement with the other data.

The strongest argument in favor of model I is the observed variation of the c cell parameter and z coordinate of the various ions with the Li substitution. (These parameters are deduced from the refinement of the 3T2 neutron spectra but are independent of the assumed model.) It appears that the substitution has no effect on the a cell parameter but entails a decrease of c which results from the decrease of z(O2). This z(O2) decrease is remarkable, compared to the slight increase of z(Cu2) (see Fig. 8). We interpret it as due to the suppression of the repulsive interactions between the O2 ions and the apical oxygens that have been shifted to chain sites. This displacement also gives rise to a slight diminution of z(Ba), at the limit of the experimental uncertainty given the dispersion of the literature data, which is due to an increased attractive interaction between the Ba ions and the oxygen (O4) ions in the plane $z = 0$. We thus get with this model, a coherent view of the z coordinate of the various ions, while with model II, it is difficult to explain how the Li2 substitution can lead to the observed large decrease of z(O2).

Finally, let us come back to Li-substituted orthorhombic $YBa_2Cu_3O_7$. The c decrease that we observed in our $YBa_2Cu_{3-x}Li_xO_{7-x}$ samples is the more remarkable as the oxygen loss which goes with the Li substitution should produce, were chain oxygens lost, an increase of c. This and a number of other reasons [6] show that one apical and not chain oxygen is lost per substituted Li. Then the question is: how is the electrical neutrality preserved if Li^+ substitutes for $Cu2^{2+} + O1^{2-}$, without any hole being lost? We suggest that, in $YBa_2Cu_{3-x}Li_xO_{7+x}$ as in $YBa_2Cu_{3-x}Li_xO_6$, the O1 vacancy may be surrounded by a Li^+ and a $Cu1^+$. The substitution would then write $Cu2^{2+} + O1^{2-} + Cu1^{2+} \rightarrow Li2^+ + Cu1^+$, and not affect the hole number.

6 Conclusion

The aim of the present experiment was to ascertain the origin of the holes responsible for the suppression of the AF order in Li-substituted $YBa_2Cu_3O_6$: were they, as expected, created in the CuO_2 planes by the substitution $Cu2^{2+} \rightarrow Li2^+$ or could they arise from a few residual chain oxygens sitting preferentially near a $Cu1^{2+}$ or a $Li1^+$?

The present experiment shows that they do arise from the $Cu2^{2+} \rightarrow Li2^+$ substitution and not from residual chain oxygens. The Li substitution creates holes in the CuO_2 planes of tetragonal undoped $YBa_2Cu_3O_6$ and these holes are responsible for a strong suppression of the AF order. As a consequence, the suppression rate of the ordering temperature, $A = -(\Delta T_N/\Delta x)/T_N$, where x here is the fraction of replaced Cu2, is not constant, as when the suppression results from dilution only, but increases rapidly with x: $A \approx 6$–7.5 for $x = 3$–4% and $A \approx 8$–9 for $x = 4.5$–5% while A has a much smaller constant value, $A \approx 3$, for Zn [24].

The mean ordered magnetic moment is decreased proportionally to T_N , as in doped $YBa_2Cu_3O_6$.

The effect of the Li-holes on T_N and μ is quantitatively comparable to that of mobile doped holes.

Besides, the neutron data indicate that one apical oxygen is removed per substituted Li, in tetragonal $YBa_2Cu_3O_6$ as in orthorhombic $YBa_2Cu_3O_7$. If one relies on this indication, it results from the present neutron data that in tetragonal $YBa_2Cu_{3-x}Li_xO_{6+\varepsilon}$, each of these apical oxygen vacancies is surrounded by a $Li2^+$ and a $Cu1^+$. The assumption that the same configuration stands

Table 3. Schematic diagram of the local crystallographic structure of YBaCuO6 and YBaCuO7, unsubstituted and Li-substituted. A $y = 0$ plane is represented. The black spheres represent the Cu/Li ions, the gray spheres the oxygen ions, the squares the oxygen vacancies and **p** here the extra hole brought in by the substitution. Note that the neutron data do not allow to determine the exact position of the Li ions [6]. In YBaCuO6, whatever the model, one extra hole is introduced per Li ion. In contrast, no extra hole is introduced in YBaCuO7.

	$YBa_2Cu_3O_y$	$YBa_2Cu_{3-x}Li_xO_y$
y = 6 Model II	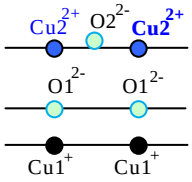	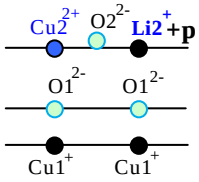
y = 6 Model I	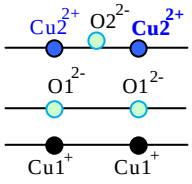	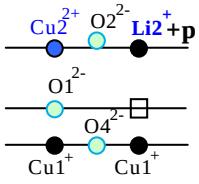
y = 7	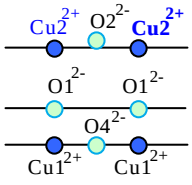	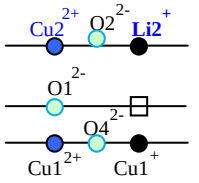

in orthorhombic $YBa_2Cu_{3-x}Li_xO_{7-x}$, then explains why in this compound, the Li substitution does not modify the hole concentration in the CuO_2 planes.

Table 3 illustrates schematically the present conclusion.

References

1. J.M. Tranquada, D.E. Cox, W. Kunnmann, H. Moudden, G. Shirane, M. Suenaga, P. Zolliker, D. Vaknin, S.K. Sinha, M.S. Alvarez, A.J. Jacobson, D.C. Johnston, Phys. Rev. Lett. **60**, 156 (1988).
2. P. Burlet, C. Vettier, M.J. Jurgens, J.Y. Henry, J. Rossad-Mignod, H. Noel, M. Potel, P. Gougeon, J.C. Levet, Physica C **153-155**, 1115 (1988).
3. F. Maury, M. Nicolas-Francillon, I. Mirebeau, F. Bourée, Physica C **353**, 93 (2001).
4. J. Bobroff, W.A. MacFarlane, H. Alloul, P. Mendels, N. Blanchard, G. Collin, J.F. Marucco, Phys. Rev. Lett. **83**, 4381 (1999)
5. M. Nicolas-Francillon, F. Maury, R. Ollitrault-Fichet, M. Nanot, P. Legeay, J. Appl. Phys. **84**, 925 (1998).
6. F. Maury, M. Nicolas-Francillon, F. Bourée, R. Ollitrault-Fichet, M. Nanot, Physica C **333**, 121 (2000).
7. J. Rodriguez-Carjaval, *Abstract Sat. Meeting on Powder Diffraction*, IUCr. Conf., Toulouse (1990), p. 127
8. F.C. Fritschij, H.B. Brom, R. Berger, Solid State Commun. **107**, 719 (1998).
9. M.A.G. Aranda, J.P. Attfield, Angew. Chem. Int. Ed. Engl. **32**, 1454 (1993).
10. R. Hoffmann, R. Hoppe, W. Schäfer, Z. Anorg. Allg. Chem. **578**, 18 (1989).
11. S. Zagoulev, P. Monod, J. Jégoudez, Phys. Rev. B **52**, 10474 (1995).
12. D.C. Johnston, A.J. Jacobson, J.M. Newsam, J.T. Lewandowski, D.P. Goshorn, D. Xie, W.B. Yelon, *Chemistry of Hign Temperature Superconductors*, Chap. 14 (AMS, Washington DC, 1987), p. 136.
13. J.D. Jorgensen, B.W. Veal, A.P. Paulikas, L.J. Nowicki, G.W. Crabtree, H. Claus, W.K. Kwok, Phys. Rev. B **41**, 1863 (1990).
14. H. Casalta, P. Schleger, P. Harris, B. Lebech, N. H. Andersen, Ruixing Liang, P. Dosanjh, W.N. Hardy, Physica C **258**, 321 (1996).
15. J. Rossat-Mignot *et al.*, J. Phys. Colloq. France **49**, C8-2119 (1988).
16. Y. Sidis, P. Bourges, B. Hennion, R. Villeneuve, G. Collin, J.F. Marucco, Physica C **235-240**, 1591 (1994).
17. M. Corti, A. Rigamonti, F. Tabak, P. Caretta, F. Licci, L. Raffo, Phys. Rev. B **52**, 4226 (1995).
18. B. Keimer, A. Aharony, A. Auerbach, R.J. Birgeneau, A. Cassanho, Y. Endoh, R.W. Erwin, M.A. Kastner, G.H. Shirane, Phys. Rev. B **45**, 7430 (1992)
19. G. Uimin and J. Rossat-Mignot, Physica C 199 (1992) 251.
20. H. Tolentino, F. Baudelet, A. Fontaine, T. Gourieux, G. Krill, J.Y. Henry, J. Rossat-Mignod, Physica C **192**, 115 (1992).
21. Y. Sidis, private communication.
22. J.M. Tranquada, A.H. Moudden, A.I. Goldman, P. Zolliker, D.E. Cox, G. Shirane, S.K. Sinha, D. Vaknin, D.C. Johnston, M.S. Alvarez, A.J. Jacobson, Phys. Rev. B **38**, 2477 (1988).
23. J.H. Brewer *et al.*, Phys. Rev. Lett. **60**, 1073 (1988).
24. Y. Sidis, P. Bourges, B. Hennion, R. Villeneuve, G. Collin, J.F. Marucco (to be published).